PROCEEDINGS, Twenty-First Workshop on Geothermal Reservoir Engineering
Stanford University, Stanford, California, January 22-24, 1996
SGP-TR-151

PERMEABILITY DECREASE IN ARGILLACEOUS SANDSTONE; EXPERIMENTS AND MODELLING

Paul Egberts(*), Lennard van Soest(**), Jean-François Vernoux(***)

(*) TNO Institute of Applied Geoscience
P.O. Box 6012, 2600 JA Delft
The Netherlands

(**) Technical University Delft
P.O. Box 5028, 2600 GA Delft
The Netherlands

(***) BRGM
P.O. Box 6009, 45060 Orleans cedex 2
France

ABSTRACT

Core flooding experiments on argillaceous sandstone are carried out showing that for high injection flow rates permeability reduction occurs. The decrease of permeability is a consequence of the migration of in-situ particles. Two models are used to simulate the observed phenomena. The so-called network model is able to give insight in the physics behind the particle migration. The other model based on mass balance and constitutive laws is used for quantitative and qualitative comparison with the experiments.

1. INTRODUCTION

With the exploration and development of significant geothermal resources stored in clastics deposits, widespread in Europe, serious formation injectivity problems were experienced (Ungemach, 1983). Previous studies showed that the particles of geothermal fluid and the particles of rock matrix can induce a strong permeability decrease (Ochi and Vernoux, 1994; Vernoux and Ochi, 1994; Boisdet et al., 1987). The invasion of the reservoir by the particles contained in the geothermal fluid can be limited by ad hoc surface installation. But in the reservoir near the well wall, the high velocities can induce mechanical phenomena like particle release. In that case the risks of formation damage cannot be predicted without a detailed understanding of the physical phenomena.

A probable reason for injectivity decline is the release and subsequent deposit of internal particles. Two causes can be distinguished for the release of internal particles. Firstly, particles are released due to a repulsive interaction force with respect to the porous matrix. The interaction force depends on the salinity of the brine and can become repulsive if the salinity is sufficiently low. This phenomenon of a decreasing permeability due to a change of salinity is known as the water sensitivity of sandstone and has been described by Khilar and Folger (1983). Secondly, internal particles are released when the hydrodynamic force overcomes an attractive interaction force between particles and the grains. This mechanism is in particular of interest for this study because of the high injection rates common for geothermal doublets.

In the next section we will discuss laboratory experiments which demonstrate the permeability decline due to the migration of internal particles. The influence of salinity and injection rate will be explained briefly. For a more extensive discussion we refer to Ochi and Vernoux (1994).

In Section 3 we present some simulations of permeability decline using a network model. In this model the porous medium is considered to be a network of pores interconnected by tubes with different radii. Initially, the pores are randomly filled with an amount of internal particles. By computing the local velocity in a pore and using a rate law, a certain amount of the internal particles will be released. The deposit is now modelled by changing the adjacent radii of the pore according to the amount of released particles. An important advantage of such a network model is the ability to take into account the physics on the pore level and hence give insight in the different deposition mechanisms such as size exclusion and surface deposition.

The model we use in Section 4 is acting on a larger scale than the network model i.e. the core scale. It is based on mass balance, Darcy's law and constitutive

laws for the internal particles and deposit. In this model the porous medium is considered as a filter for the suspended particles. In principle the model allows for suspended particles both from external origin or from release of internal particles. However, in this paper we consider only the case of internal particles, that is, the injection fluid is solid-free. A fundamental law relating the deposit and the concentration of the particles in the fluid is taken from filtration theory. The model describes the evolution of the deposit. To determine the effect of the evolution of the deposit on the behaviour of the permeability, knowledge is needed on how the permeability depends on the deposit. In the literature several empirical relations are proposed for the dependence of the permeability on the deposit (Gruesbeck and Collins 1982). We will indicate how the network model could also be used to provide such a relationship. The model is coupled with an optimisation routine in order to calibrate the model.

2. LABORATORY EXPERIMENTS

Results

All experiments were carried out on Berea sandstone plugs and with solid-free brines. During some of the experiments the flow rate is stepwise increased. Furthermore, experiments are performed with different salinity. The pressure difference over the plug is measured during the core flooding test. The permeability is computed using Darcy's law.

The following table summarises the experimental conditions.

Exp	fluid (M NaCl)	flow rate (cm^3/s)	PV (10^3)	permeability (mD)
BS013	0.01	1 -> 7	4.8	330 -> 160
BS012	0.1	2 -> 14	14	340 -> 190
BS011	0.5	3.6 -> 14.5	20.5	480 -> 280
BS010	0.5 ->0	1.2 -> 5.4	5	430 -> 100
g-22-08	0.5	4.1	17.5	440 -> 340
g-24-08	0.5	6.9	12	440 -> 280
g-31-08	0.1	6.9	18.5	500 -> 310
g-08-09	0.5 (80°C)	6.7	18	500 -> 160

Figure 2.1. Conditions and results of the experiments.

In Figure 2.2 the permeability decline of the plugs BS010-BS013 are shown.

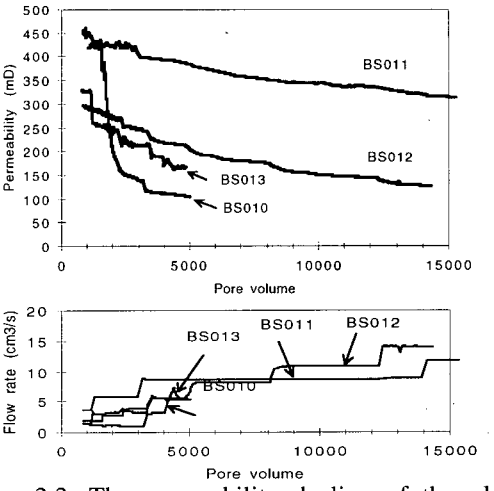

Figure 2.2. The permeability decline of the plugs BS010-BS013 and the flow rates during the core flooding experiments.

The total permeability decline is larger for lower salinity. In experiment BS010, it is observed that a rapid and large permeability decrease occurs after changing the injection fluid from 0.5 M NaCl brine to pure water. This phenomena confirms results from Khilar and Folger (1983).

The other three experiments BS011-BS013 show that an increase of the flow rate gives a sudden decrease of the permeability. After this sudden decrease, the permeability decreases steadily to an asymptotic value. We remark here, however, that in experiment BS011 the permeability reduction becomes almost linear after the increase of the flow rate to 8.3 cm^3/s and that a further increase of the flow rate does not result in a sudden decrease of the permeability. Furthermore experiment BS013 shows that initially there is no permeability reduction. Only after an increase of the flow rate from 1 cm^3/s to 3 cm^3/s a sudden and large permeability reduction is observed. For a more extensive discussion of the experiments BS010-BS013 we refer to Ochi and Vernoux (1994) and Ochi (1994).

Experiments g-22-08 and g-24-08 (see Figure 2.3) were both carried out with a constant flow rate during the injection period and the same salinity. They demonstrate that a higher flow rate results in a larger permeability decline. Comparing the experiments g-24-08 and g-31-08 it follows that the total permeability reduction is most severe for lower salinity. Experiment g-08-09 is carried out to investigate the

influence of the temperature on the permeability decline. The experiment with brine of 80 °C shows, compared with g-24-08, a larger permeability decline. Figure 2.3. The core flooding tests with a fixed flow

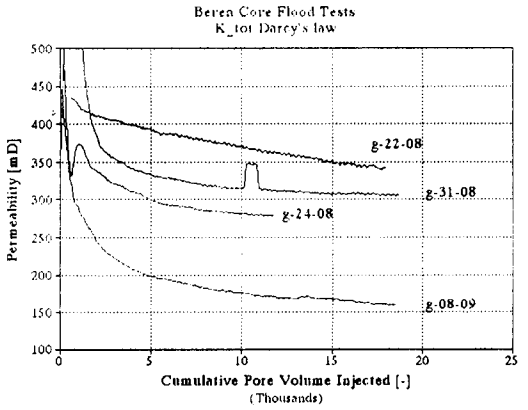

rate during the injection period.

Interpretation

From the experiments we can conclude that the total permeability reduction is most drastic for lower salinity. Furthermore a higher flow rate results in a larger permeability reduction. The phenomena observed in experiment BS010 confirms the findings of Khilar and Folger (1983), so-called the water sensitivity of sandstone. They explained the water sensitivity by showing the existence of a critical salt concentration below which the interaction between fines and the porous matrix becomes repulsive. In particular the change of the brine to pure water results in an instantaneous release of internal particles which subsequently deposit causing the permeability reduction.
The results of the core flooding tests can be explained by using DLVO theory (Ochi and Vernoux 1994; Ochi 1994). This theory enables to quantify the forces of interaction between particle and grain. The three main forces which are involved are the Van Der Waals force, electrostatic force and the hydrodynamic force. These forces can be quantified assuming a simple geometry of a sphere and a plate. The Van Der Waals force is attractive, the electrostatic force depends on the salinity and is repulsive. The hydrodynamic force is proportional to the interstitial velocity. Quantifying the resultant of the forces shows that the resultant becomes repulsive below what is called the critical salt concentration or above a critical interstitial velocity. The effect of a salinity below the critical salt concentration is shown in experiment BS010 while the notion of a critical velocity is demonstrated in experiment BS013.

Concerning the influence of the temperature on the permeability decline as shown by experiment g-08-09 we refer to the paper by Baudracco (1989). Experiments reported in that paper show that when increasing the temperature the permeability decline increases in case of a low salinity and decreases in case of a high salinity.

3. NETWORK MODEL

Model formulation

A two dimensional network model has been developed to simulate permeability decrease resulting from the detachment and capture of in situ particles in porous media (Ochi and Vernoux, 1995; Ochi, 1994). The porous network is considered as a regular lattice in which the branches represent pore throats and the nodes represent the interconnected pore bodies. In a first stage, the initial flow field into the network is computed. In a second stage, release and capture mechanisms are incorporated in the model.

Particles attached at pore walls can be released when the local velocity is greater than a critical value. Particle detachment is described by a first order kinetic equation derived from Khilar and Fogler (1983) but using a release coefficient depending on the difference between local velocity and a critical velocity.

$$r_r = -\frac{d\sigma^i}{dt} = \alpha(v_i - v_c)\sigma^i$$

After being released, the particles can be captured at the next throat entrance by different mechanisms: size exclusion, interception, diffusion. The capture of particles induces a modification of the porous network. If the particle has a radius greater than that of the output throat, then it plugs the throat. If the particle radius is lower than that of the output throat, it is captured at the throat wall. The particle capture by interception is also described by a first order kinetic equation.

$$r_c = \frac{d\sigma}{dt} = \beta c$$

where ß is the capture coefficient as defined by Khilar and Fogler (1983)

$$\beta = 1.5\,\pi\, r_p^2\, v_i\, N$$

In each branch of the network, the variation of pore throat volume is equal to the volume of captured par-

ticles, which gives the following expression for the variation of the pore throat radius

$$\frac{dr}{dt} = \frac{-1}{2\pi r L}\frac{dV_p}{dt}$$

V_p is computed from the capture equation and the mass balance on particles in each cell given by

$$\frac{dc}{dt} = r_r - r_c$$

This equation can be solved analytically. By considering the volume of suspended particles in one pore, we obtain the following expression of variation of pore throat radius

$$\frac{dr}{dt} = \frac{-\beta V_{por}}{2\pi r L}\frac{\alpha \sigma_0}{\beta - \alpha}(\exp(-\alpha t) - \exp(-\beta t))$$

At each time step the permeability is recomputed from the new radii distribution. The model also enables to compute the macroscopic rate of capture by interception from the volume of captured particles in each pore throat.

$$V_p(t) = V_{por}\sigma_0\left(1 - \frac{\alpha\exp(-\beta t) - \beta\exp(-\alpha t)}{\alpha - \beta}\right)$$

Simulation results

We now apply our model to the simulation of the percolation experiment BS013. In this experiment a critical flow rate was put in evidence between 1.5 and 3.1 cm^3/s. For a core plug with a radius of 4.5 cm and a porosity of 20%, the corresponding interstitial velocity ranges between 0.6 and 1.2 cm/s. For the simulations we used a critical velocity of 1 cm/s.

From mercury porosimetry measurements and petrography study we defined parameters used by the model to compute the initial pore throat distribution and particle distribution (Figure 3.1). The ratio between mean pore throat radius and mean particle radius is about 5/3.

The release coefficient α is the only input parameter for which we have no expression. Three simulations were carried out with three different values of α. We see in Figure 3.2 that the effect of this parameter on normalised permeability is very important. With the highest value of α, the permeability decreases even when the mean interstitial velocity is lower than critical velocity (simulation 3). This can be explained by the use of a distribution of local velocities instead of a mean interstitial velocity. For these simulations, about 1/4 of the initial local velocities are greater than 1 cm/s and then particles can be released.

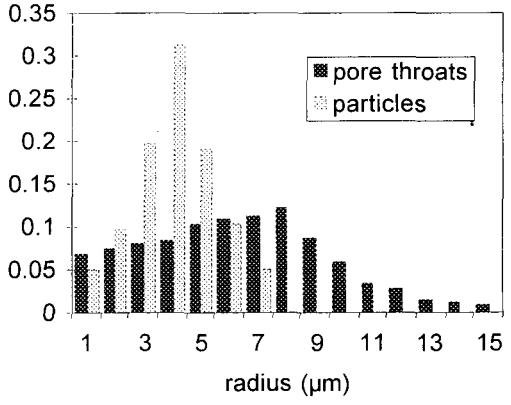

Figure 3.1. Initial distribution of pore throats and particles.

The best simulation is obtained for $\alpha = 5\ 10^{-6}$ (simulation 1). We reproduce the change of permeability evolution when increasing the flow rate but more gradually with the simulation than with the experiment. In the experiment, when the flow rate is increased, a large amount of internal particles are released on a short time period and the dominant mechanism of capture is size exclusion, that induces a sharp permeability decrease (Ochi and Vernoux, 1994). But when the particles are small the reduction in the permeability is slow since the dominant mechanism is interception.

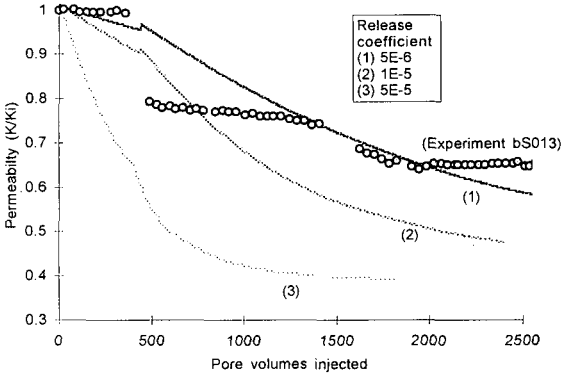

Figure 3.2. Simulation of permeability evolution by release and capture of internal particles

With the first simulation, Figure 3.3 shows that the relation between the permeability and the concentra-

tion of captured particles in non-linear. This relation, however, differs from expressions (see Section 4) reported in the literature.

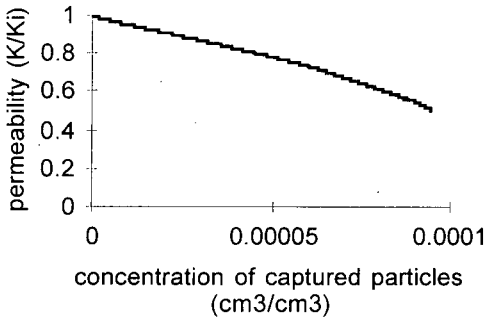

Figure 3.3. Relation between permeability and capture

4. CORE SCALE MODEL

Model formulation

In this section we describe a model for the permeability decline which is able to deal with both internal and external particles. The model consists of rate laws for the deposit and internal particles, a mass balance equation and Darcy's law. A widely accepted rate law for the deposit is given by

$$\frac{\partial \sigma}{\partial t} = v\lambda c$$

where λ is the so called filter coefficient (see e.g. Ives, 1975). The filter coefficient λ depends on the capture mechanism. Since these mechanism are not well understood, there is no complete expression for λ. Nevertheless, it is generally accepted that λ is inversely proportional to the interstitial velocity (Ives, 1975). It can be argued that there is a maximal interstitial velocity at which λ vanishes. The maximal value of the interstitial velocity can be interpreted as the velocity for which deposit and release is in balance. Taking these considerations into account we assume that λ is of the form

$$\lambda = \lambda(\sigma, v) = \lambda_0 \frac{1}{v}(1 - \frac{\sigma}{\sigma^*}) ,$$

for $0<\sigma<\sigma^*$, where the maximal deposit σ^* corresponds to the maximal interstitial velocity. The rate law for the release of the internal particles as proposed by Khilar and Folger (1983) is given by

$$\frac{\partial \sigma^i}{\partial t} = -\alpha(\sigma, v)\sigma^i$$

Following these authors, the release coefficient $\alpha=\alpha(\sigma,v)$ is taken to be proportional to the interstitial velocity. Moreover, as has been seen in Section 2, particles are released only if the interstitial velocity is above some critical value v_c. This leads to the following expression

$$\alpha = \alpha(\sigma, v) = \alpha_0(\frac{v}{\varphi - \sigma} - v_c)$$

for $v/(\varphi -\sigma) > v_c$ and $\alpha = 0$ otherwise.
The equations for the deposit and internal particles are completed by the mass balance equation

$$\frac{\partial c}{\partial t} + v\frac{\partial c}{\partial x} = -v\lambda(\sigma, v)c + \alpha(\sigma, v)\sigma$$

Darcy's law

$$\frac{\partial p}{\partial x} = -\frac{\mu}{k(\sigma)} v$$

and the appropriate boundary conditions. Under the constraint of constant flow rate during the injection period, the two rate laws plus the mass balance equation describe the evolution of the deposit. In addition, a functional relation $k = k(\sigma)$ is needed to compute the resulting permeability decline. Many relations for the permeability as function of the deposit are proposed in the literature. In Gruesbeck and Collins (1982) the empirical relations

$$k(\sigma) = k_0(1 + \beta\sigma)^{-1}$$

and

$$k(\sigma) = k_0 \exp(-\beta\sigma^4)$$

are used, for surface deposition and pore blocking respectively. In this paper we use the expression

$$k(\sigma) = k_0(1 - \beta\sigma^\gamma)$$

Note that this relation approximates the expressions for the permeability as proposed by Gruesbeck and Collins for $\gamma = 1$ and $\gamma = 4$. Because the filtration constant λ_0, the release constant α_0, the parameters β, γ and the critical velocity v_c are depending on the details of the deposition and release mechanism these parameters are difficult to asses theoretically. In order to be able to compare the simulations with the laboratory experiments we have linked the model with an optimisation routine. This routine allows for a priori upper and lower bounds for the parameters λ_0, α_0, β, γ and v_c as constraints. For instance an a priori estimate based on experiments can be given for the critical velocity v_c.

Simulation results

In figure 4.1 the result of the optimisation is given for experiment BS013. The sum of the squares of the differences of the experimental permeability data and the simulation data is optimised by varying the five above mentioned parameters. In the simulation the injection rate is increased according to the experiment (see figure 2.2). It can be concluded that the shape of permeability decrease due to the increase of the injection rate can be reproduced by the model.

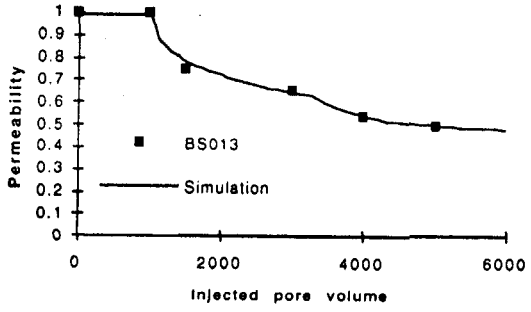

Figure 4.1. Match of experiment BS013.

Figure 4.2 shows the match of the experiments g-22-08 and g-24-08. In these experiments the difference is the injection rate. We have matched simultaneously both experiments, that is, the simulations of both experiments as shown in the figure have the same parameter values and an injection rate according to the experiments.

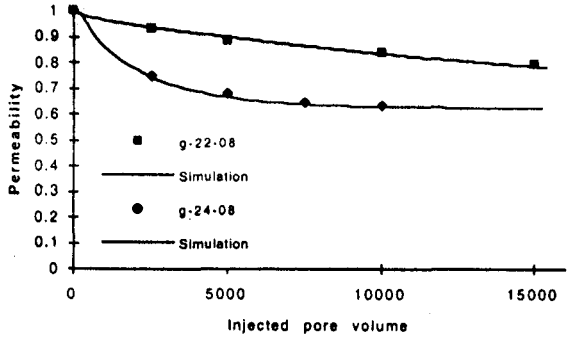

Figure 4.2. Simultaneous match of the experiments g-22-08 and g-24-08.

CONCLUSIONS

The laboratory investigations demonstrates that high flow rate injection causes a permeability decrease. Increasing the flow rate induces a more severe permeability decline. Furthermore, the salinity of the injection fluid influences the degree of the permeability reduction; low salinity results in a larger reduction of the permeability. The observed permeability decline is due to the deposition of the released internal particles. By means of the DLVO theory, it can be argued that above a critical interstitial velocity or below a critical salt concentration internal particles are released. The notion of a critical interstitial velocity is demonstrated in experiment BS013. The consequence of a salinity below the critical salt concentration can be seen in experiment BS010.

In order to understand in more detail the observed phenomena of permeability decline, two models have been developed. A model based on network theory simulates the clogging of a porous medium by in-situ particles release and capture. This model is able to study the release and deposition mechanism in detail and how these mechanisms influences the permeability. The model takes into account three mechanisms of capture (size exclusion, interception and diffusion) and a real distribution of flow velocities. The curves of simulated permeability have the same shape as experimental curves but the model does not accurately simulates the sharp permeability decrease when a large amount of particles are captured on a short time step. This phenomenon is observed experimentally when increasing the flow rate over a critical value. The interest of this model is to put in evidence of complex physical phenomena at local scale and to simulate the gradual clogging of the porous medium without semi-empirical relations.

In the core scale model the release and deposition mechanism are represented in the filtration coefficient $\lambda(\sigma)$, the release coefficient $\alpha(\sigma)$ and the expression $k(\sigma)$ for the permeability. As an example of upscaling from pore to core scale, it has been demonstrated how the network model based on pore scale physics leads to a functional relation $k = k(\sigma)$ (Figure 3.3). This relation can serve as input for the core scale model.

The core scale model can reproduce the core flooding experiments qualitatively. By using an optimisation routine the model can be calibrated. The optimisation parameters are the parameters in the expressions for the filtration and release coefficient and the expression for the permeability. The method of optimisation we use is able to deal with constraints. Thus, knowledge of the range of a parameter can be taken into account to obtain physically sensible values for the

parameters.
Simultaneously with the core scale model a radially symmetric version has been developed. The radially symmetric model can be regarded as a model on bore-hole scale. An important difference between the core and bore-hole scale model is that for the latter, the interstitial velocity is inversely proportional to the distance from the injection well. As indicated above by matching the core scale model and the core flooding experiments values for the optimisation parameters are obtained. These values in turn serve as input for the bore hole scale model. In the near future we will investigate differences between the core and bore-hole scale model. Furthermore, we intend to study the ability of these models to predict the behaviour of the permeability on the long term.

NOTATION

[L]: Length unit, [T]: Time unit, [M]: Mass unit.

A:	Cross sectional area [L^{-2}]
α:	Release coefficient [L^{-1}]
α_0:	Release constant [L^{-1}]
c:	Concentration [-]
φ:	Porosity [-]
k:	Permeability [L^2]
k_0:	Initial permeability [L^2]
L:	Pore throat length [L]
λ_0:	Filtration constant [T^{-1}]
μ:	Viscosity [$ML^{-1}T^{-1}$]
N:	Number of collectors per unit volume [-]
p:	Pressure [$ML^{-1}T^{-2}$]
q:	Flow rate [$L3T^{-1}$]
r:	Pore throat radius [L]
r_r:	Rate of release [T^{-1}]
r_c:	Rate of capture [T^{-1}]
r_p:	Particle radius [L]
σ:	Deposit [-]
σ^*:	Maximal deposit [-]
σ^i:	Internal particles [-]
σ_0:	Initial concentration of particles on pore walls [-]
t:	Time [T]
v:	Darcy velocity q/A [LT^{-1}]
v_c:	Critical interstitial velocity [LT^{-1}]
v_i:	Local velocity [LT^{-1}]
V_p:	Volume of captured particles [L^3]
V_{por}:	Pore volume [L^3]

ACKNOWLEDGEMENT
This research has been funded by the European Commission and the Netherlands agency for energy and the environment Novem, in the framework of the JOULE II Programme, Sub-programme Non Nuclear Energy.

REFERENCES
Boisdet, A., Cautru, J.P., Czernickowski-Lauriol, I., Foucher, J.C., Fouillac, C., Honegger, J.L., and Martin, J.C., (1989), "Experiments on reinjection of geothermal brines in the deep triassic sandstones," In: European Geothermal Update, K. Louwrier, E. Staroste, J.D. Garnish and V. Karkoulias (Eds), Kluwer Science Publishers, Dordrecht, 419-428.

Baudracco J., (1989), "Variations of the permeability and fine particle migrations in unconsolidated sandstone submitted to saline circulations," Water-Rock Interaction, Miles (ed), 49-53.

Gruesbeck C. and Collins R.E., (1982), "Entrainment and deposition of fine particles in porous media," SPEJ, Vol. 22, n°6, 847-856.

Ives K.J., (1975), " Mathematical models of deep bed filtration," In: The scientific basis of filtration, K.J. Ives (ed), Noordhoff, Leiden 1975.

Khilar, K.C. and Folger, H.S. (1983), "Water sensitivity of sandstones," SPE Journal, 55-64.

Ochi, J. (1994) "Etude et modelisation de la chute de permeability en relation avec l'injection de fluides dans les reservoirs argilo-greseux," Ph. D. thesis, university of d'Orsay.

Ochi, J. and Vernoux, J.F. (1994), "Origin of permeability reduction in high flow rate injections," Int. Symp. on the Scientific and Engineering Aspects of Deep Injection Disposal of Hazardous and Industrial Wastes, Lawrence Berkeley Laboratory, May 10-13, in press.

Ochi J. and Vernoux J.F. (1995), "A two dimensional network model for simulating permeability decrease during fluid injection into aquifers." Groundwater quality: Remediation and protection. Int. Conf. held at Prague, Czech Republic, 15-18 May.

Ungemach P. (1983), "Drilling, production, well completion and injection in fine grained sedimentary reservoirs with special reference to reinjection of heat depleted geothermal brines in clastic deposits." Report of an extended contractors meeting held in Brussels on 23 March 1983.

Vernoux J.F. and Ochi J. (1994), "Aspects relative to the release and deposition of fines and their influence on the injectivity decrease of a clastic reservoir." Geothermics 94 in Europe, Int. Symp. held in Orléans, France, 8-9 Feb., 291-302.